Supporting Information for "Satellite-Observed Vegetation Responses to Intraseasonal Precipitation Variability"

Bethan L. Harris[1,2], Christopher M. Taylor[1,2], Graham P. Weedon[3], Joshua Talib[1], Wouter Dorigo[4], Robin van der Schalie[5]

[1]UK Centre for Ecology & Hydrology, Wallingford, UK

[2]National Centre for Earth Observation, Wallingford, UK

[3]Met Office, Wallingford, UK

[4]Department of Geodesy and Geoinformation, TU Wien, Vienna, Austria

[5]Planet, Haarlem, the Netherlands

Contents of this file

1. Text S1
2. Figures S1 to S4

References

Moron, V., & Robertson, A. W. (2020). Tropical rainfall subseasonal-to-seasonal predictability types. *npj Climate and Atmospheric Science*, *3*(1). doi: 10.1038/s41612-020-0107-3

Text S1: Inundation masking Since artificial decreases in VOD due to inundation tend to coincide with increases in SSM, we first compute the linear trends over a 7-day rolling window in both VOD and SSM. Where VOD trends lying within the low tail of the climatological distribution coincide with SSM trends in the high tail of its distribution, we mask the whole 7-day window as a "surface water event". We found that choosing thresholds of 15% (lower) and 85% (upper) to define the tails of the distributions removed the vast majority of inundation cases, whilst maintaining sufficient data points for global analysis. We also exclude weeks with low-tail VOD trends and fewer than three SSM observations, to avoid missing inundation when it is not possible to observe the associated high-tail SSM trend. This part of the approach tends to over-mask data in tropical rainforests, where there are no SSM observations, but our priority was to remove pixels in which inundation might lead to us drawing spurious conclusions about the relationship between precipitation and vegetation. Tropical rainforest pixels mostly do not exhibit coherent relationships even if the cross-spectral analysis is run without performing inundation masking first (not shown).

As inundation effects can persist for several weeks after the initial wetting, we include a second mask using the SWAMPS surface water fraction. We compute correlations between weekly VOD and water fraction over a 25-day rolling window and extend each surface water event until there is no significant ($p < 0.1$) negative correlation for 7 days in a row. This masks increases in VOD as inundation recedes. An example of the masking procedure is illustrated in Figure S1. Maps of the pixels that are excluded from analysis due to inundation are found in Figure S2.

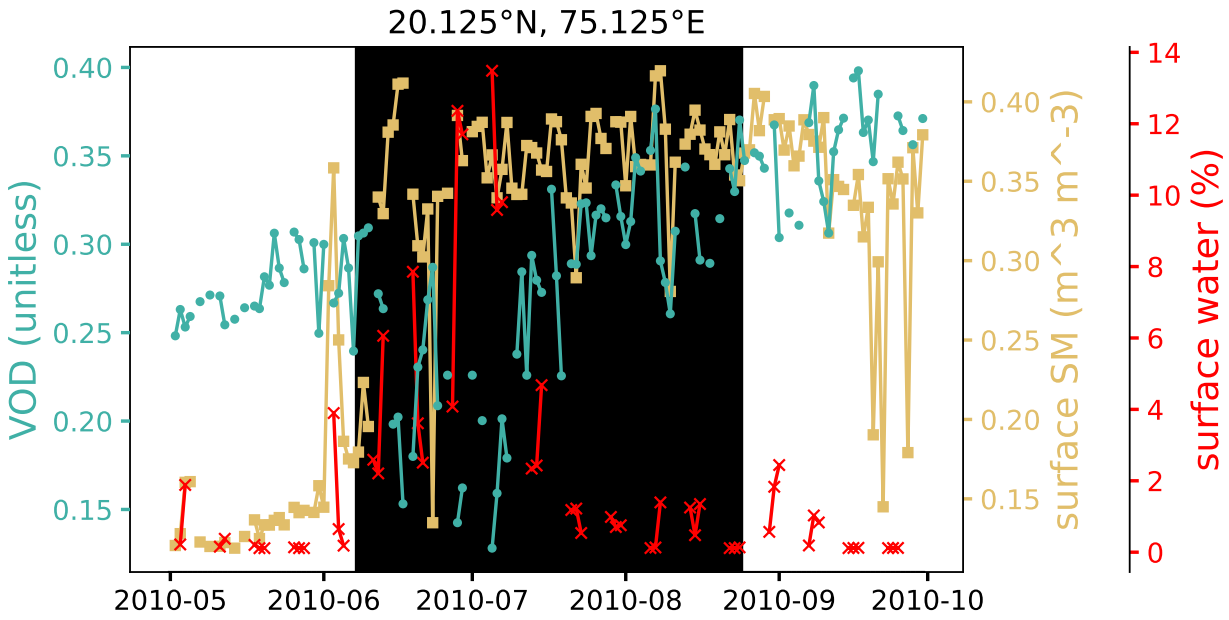

Figure S1. Example of masking VOD data to remove changes caused by inundation, as described in Section 2.1 and Text S1. This time series is taken from a cropland pixel in India. The black background shading marks days that are identified as affected by surface water changes and therefore removed from the analysis. Here, the decrease in VOD and increase in surface soil moisture occurring in mid-June are clearly associated with inundation identified by the SWAMPS dataset. VOD increases as inundation recedes over the course of the following 1–2 months, so data are masked until near the end of August.

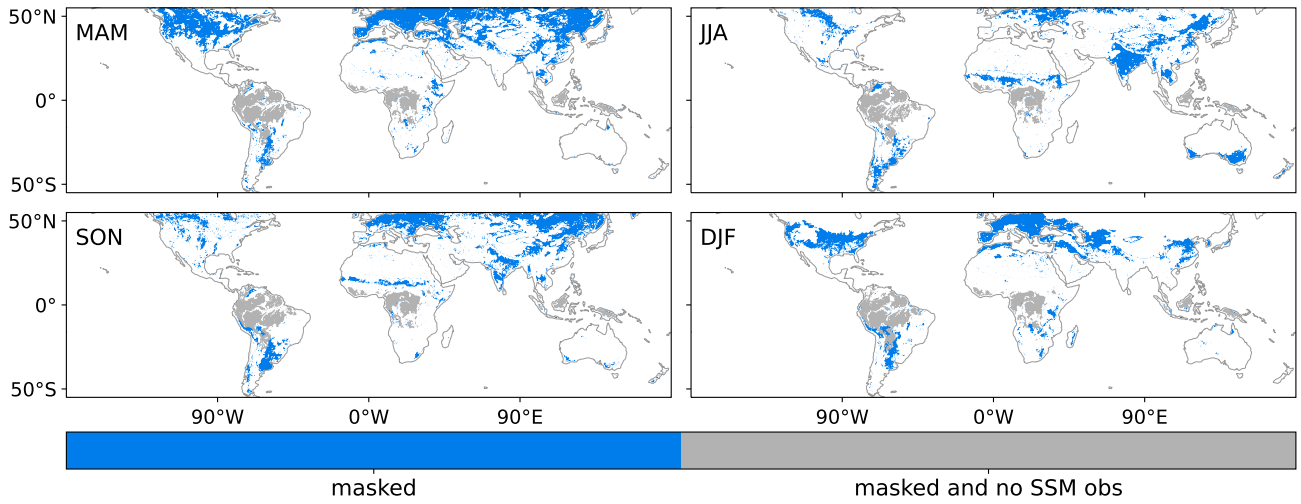

Figure S2. Pixels removed by inundation masking in each season. Both blue and grey pixels had sufficient observations for analysis (> 30% of days) before inundation masking, but insufficient observations once inundation masking was applied. In grey pixels, there are no ESA CCI SM observations, so it is likely that the procedure over-masks due to an inability to identify surface water dynamics as precisely as in blue pixels.

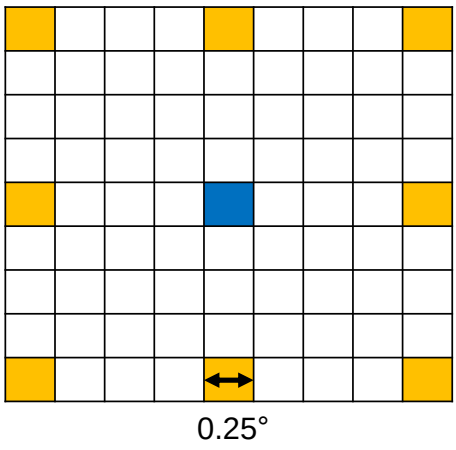

Figure S3. Pixel "neighbours" used to assess significance of coherent relationships.

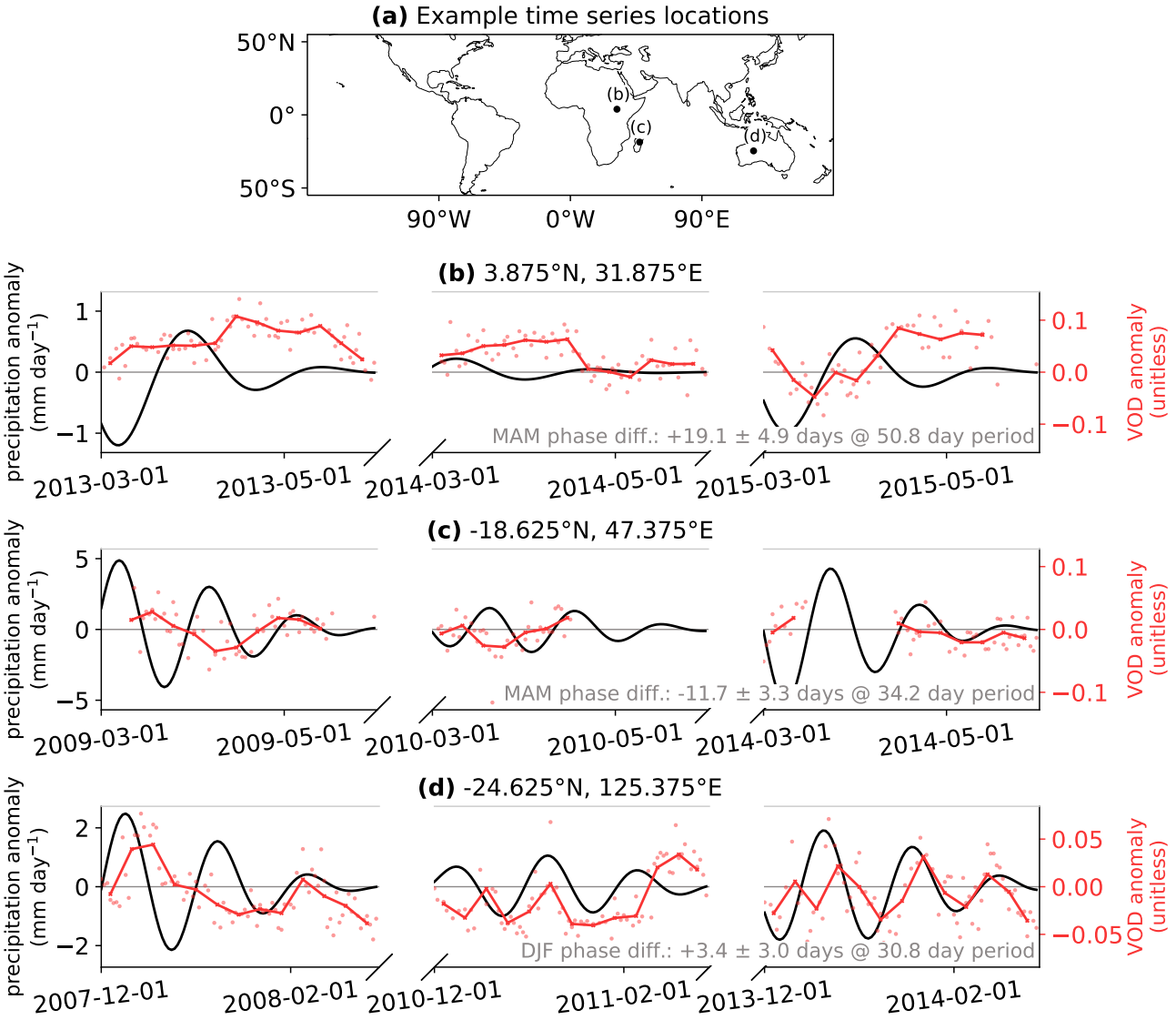

Figure S4. Time series of IMERG precipitation and VOD day-of-year anomalies for example locations. (a) Map showing the location of each set of example time series. (b-d) Time series at the location shown in the title. Precipitation anomalies (black lines) are filtered to the relevant intraseasonal variability band (40—60 days for (b), 25—40 days for (c, d)) using a Butterworth bandpass filter. Red points show daily VOD observations, while the red lines show 7-day mean values to facilitate comparison with the precipitation intraseasonal variability. The lower right-hand text in (b)-(d) shows the phase difference and period of the relationship between precipitation and VOD, as displayed in Figure 2.

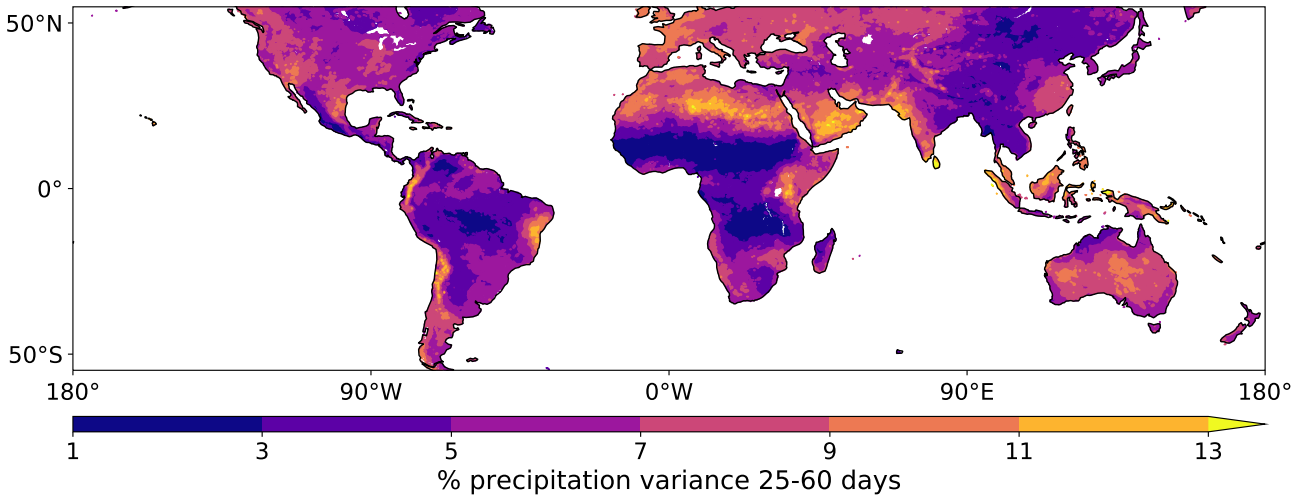

Figure S5. Percentage of total precipitation variance occurring in 25–60 day periods of variability. Computed following the method of Moron and Robertson (2020): first the square root of the IMERG data is taken, to reduce skewness, then day-of-year anomalies are computed. The anomaly time series is passed through a 25–60 day Butterworth filter, and the variance of this resulting time series is compared to the variance of the unfiltered daily anomalies.

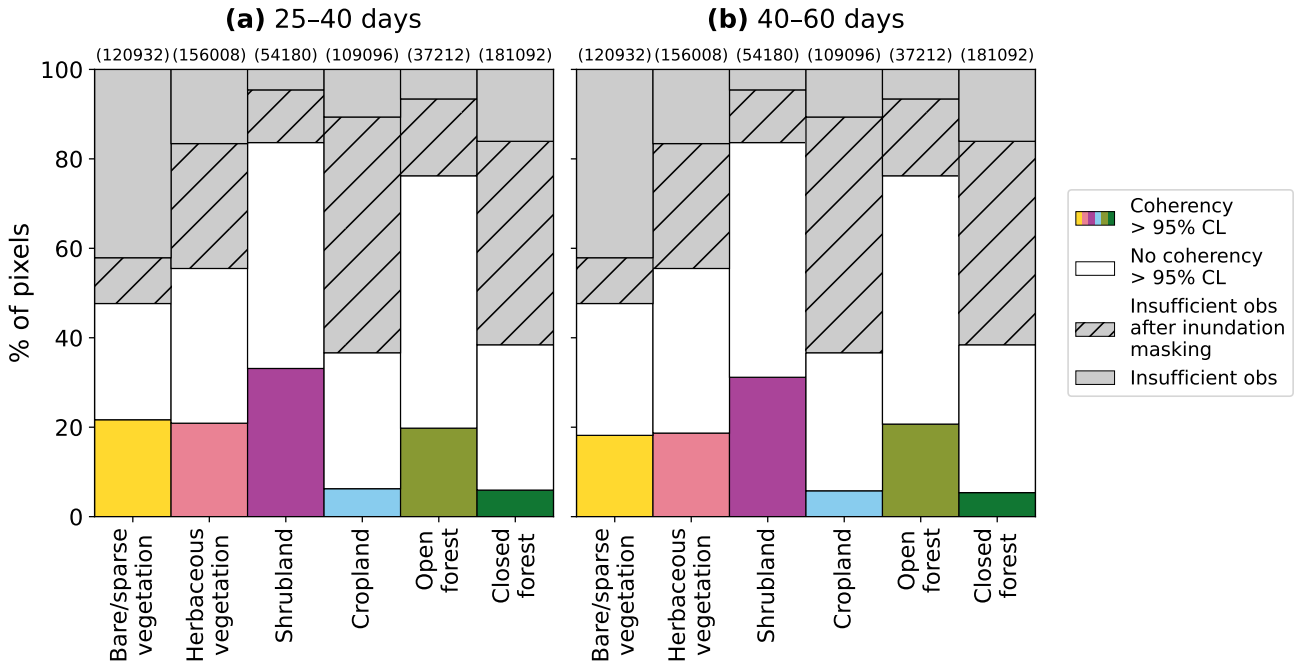

Figure S6. Percentage of pixels of each land cover with coherent intraseasonal precipitation-VOD relationships. Coloured bars show the percentage of pixels for which a 95% significant coherent relationship is observed at some period of variability between (a) 25–40 and (b) 40–60 days. White bars show the percentage for which cross-spectral analysis is performed but no significant relationship is found, and grey bars the percentage for which there are insufficient observations ($<$ 30% of days) to perform cross-spectral analysis. The hatched section of the grey bar shows the percentage for which there were sufficient observations prior to inundation masking, but insufficient observations once the masking was performed. All four seasons are included (i.e. each 0.25° pixel is counted 4 times). Numbers in brackets above bars give the total number of pixels considered for each land cover. See Figure 3a for a corresponding land cover map.